

MambaFlow: A Mamba-Centric Architecture for End-to-End Optical Flow Estimation

Juntian Du¹ Yuan Sun¹ Zhihu Zhou¹ Pinyi Chen¹ Runzhe Zhang¹ Keji Mao¹

¹College of Computer Science and Technology College of Software, Zhejiang University of Technology, China

{djt, 221124120198, zhouchi, chenpinyi, maokeji}@zjut.edu.cn mupamupa0.0@gmail.com

Abstract

Optical flow estimation based on deep learning, particularly the recently proposed top-performing methods that incorporate the Transformer, has demonstrated impressive performance, due to the Transformer’s powerful global modeling capabilities. However, the quadratic computational complexity of attention mechanism in the Transformers results in time-consuming training and inference. To alleviate these issues, we propose a novel MambaFlow framework that leverages the high accuracy and efficiency of Mamba architecture to capture features with local correlation while preserving its global information, achieving remarkable performance. To the best of our knowledge, the proposed method is the first Mamba-centric architecture for end-to-end optical flow estimation. It comprises two primary contributed components, both of which are Mamba-centric: a feature enhancement Mamba (FEM) module designed to optimize feature representation quality and a flow propagation Mamba (FPM) module engineered to address occlusion issues by facilitate effective flow information dissemination. Extensive experiments demonstrate that our approach achieves state-of-the-art results, despite encountering occluded regions. On the Sintel benchmark, MambaFlow achieves an EPE all of 1.60, surpassing the leading 1.74 of GMFlow. Additionally, MambaFlow significantly improves inference speed with a runtime of 0.113 seconds, making it 18% faster than GMFlow. The source code will be made publicly available upon acceptance of the paper.

1. Introduction

Optical flow estimation, a fundamental problem in computer vision, aims to compute the motion vectors of pixels between consecutive frames in a video sequence. Optical flow estimation holds significant and widespread applications in areas such as action recognition [37, 42], video interpolation [11, 19, 34], and autonomous driving [38].

Architectures based on Convolutional Neural Networks

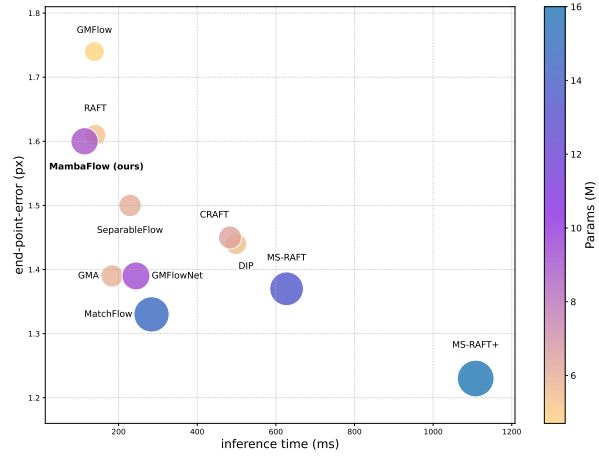


Figure 1. **End-point-error on Sintel (clean) vs. inference time (ms) and model params (M).** All models were trained on FlyingChairs (C), FlyingThings3D (T), Sintel (S), KITTI (K), and HD1K (H) datasets, with testing performed using one NVIDIA GeForce RTX 3090 GPU. Compared to state-of-the-art models, our proposed model achieves comparable accuracy while significantly reducing inference time, demonstrating an optimal balance between computational efficiency and performance.

(CNNs) have achieved pioneering progress in the field of optical flow estimation. FlowNet [4], as the first end-to-end CNNs-based flow network, revealed the immense potential of this learning paradigm. However, it faced limitations in handling large displacements and complex motions, along with high computational costs. Subsequently, PWC-Net [30] improved estimation accuracy in complex motion scenarios by incorporating pyramid feature extraction and a cost-volume construction, which effectively captured multi-scale local features. Nevertheless, it still encountered challenges in large displacement scenarios. To address these issues further, RAFT [31] introduced a recurrent iterative refinement mechanism, significantly enhancing the accuracy of optical flow estimation. Still, its optimization process relies on numerous iterations, leading to increased parameter counts and substantially longer inference time.

In recent years, the Transformer architecture, with its powerful global modeling capabilities, has been introduced into optical flow estimation tasks. For instance, GM-Flow [36] and FlowFormer [10] leverage attention mechanisms to capture long-range dependencies, significantly improving the accuracy of optical flow estimation. However, the quadratic computational complexity of the Transformers significantly increases the inference time in high-resolution scenarios, severely limiting their efficiency in practical applications. This raises a critical question: *How can we achieve efficient optical flow estimation with reduced computational overhead while preserving high accuracy?*

Mamba [5], rooted in state space models (SSMs)[6], employs an efficient selective state space mechanism to excel in tasks requiring the integration of global information and handling complex spatiotemporal dependencies. Simultaneously, it achieves linear computational complexity when capturing long-range dependencies in sequences. Inspired, we propose a novel optical flow estimation framework, MambaFlow, designed to address the challenges of large displacements, occlusions, and computational efficiency. As demonstrated in Fig. 1, our method significantly reduces inference time while maintaining high accuracy. The framework introduces two core innovations: a feature enhancement Mamba (FEM) module, which optimizes feature representations to enhance global matching performance, and a flow propagation Mamba (FPM) module, which propagates flow information to tackle challenges in occluded regions.

Specifically, our framework begins with a CNN backbone to extract robust features from the input image pair. We then propose the FEM module, which employs the Self-Mamba and Cross-Mamba mechanisms to strengthen the correlations between the extracted features, allowing for the capture of complex global information and long-range dependencies. Building on the enhanced features provided, a global matching module compute similarities and perform global optimization, to generate initial flow. This process fully utilizes global information, effectively tackling the challenges posed by large displacements. At last, we propose a Mamba-centric flow propagation method, the FPM module, which leverages feature similarity to guide propagation and produce the final accurate flow [36], tackling the occlusion issue in predicting optical flow.

Our main contributions can be summarized as follows:

- We propose MambaFlow, a novel optical flow estimation architecture built on the Mamba framework. To the best of our knowledge, this is the first Mamba-centric architecture designed for end-to-end optical flow estimation. Our method achieves comparable accuracy to state-of-the-art algorithms while significantly reducing inference time. With a runtime of 0.113 seconds, our method is 18% faster than GMFlow and 10 times faster than MS-

RAFT+.

- We introduce a feature enhancement Mamba (FEM) module, which integrates Self-Mamba and Cross-Mamba mechanisms to address insufficient feature representation. This module established a new Mamba-centric paradigm for accurate and efficient feature enhancement.
- We design a flow propagation Mamba (FPM) module for flow propagation that utilizes feature self-similarity to guide the final flow estimation. This module tackles the poor performance in recurrent refined methods by effectively propagating flow information, offering significant potential to enhance accuracy and speed, both currently and in the foreseeable future.

2. Related Work

2.1. Optical Flow Estimation

The optical flow problem is traditionally approached as an energy minimization task. Based on the assumptions of brightness constancy and spatial smoothness, Horn and Schunck [8] introduced a variational method to tackle this problem. The following studies refined optical flow estimation by framing it as an optimization problem, improving accuracy and robustness through regularization that maximizes the visual similarity between corresponding pixels in the image. In the era of deep learning, following the introduction of FlowNet [4] as the first CNN-based optical flow method, numerous subsequent algorithms such as PWC-Net [30] and SpyNet [28], adopted a coarse-to-fine strategy for optical flow estimation. However, small displacements of fast movement were often missed via the inaccurate flow guidance at the coarse level. To overcome this obstacle, RAFT [31] proposed an iterative refinement method using full-field, achieving significant improvements. Constructing upon the innovation of RAFT, later works such as GMA [15] improved the handling of occluded regions by introducing a global motion aggregation module. Similarly, SeparableFlow [40] introduced a separable cost volume module that used a global motion aggregation layer to utilize global contextual cues and prior knowledge to resolve motion ambiguity in regions. Despite the advancements, CNN-based models, including those built upon the RAFT framework, still rely on multiple iterations of refinement to achieve high-precision optical flow estimation. This iterative process significantly increases computational overhead and slows inference speed, thereby limiting their practicality for efficiency-sensitive applications.

In recent years, the Transformer architecture has demonstrated exceptional proficiency in modeling long-range dependencies and global information through its self-attention mechanism, making it a popular choice for optical flow estimation tasks. By incorporating more global and contextual information, it has significantly improved estimation

accuracy. FlowFormer [10] further optimized model performance by encoding 4D cost tags into cost memory and applying alternating groups of Transformer layers in the latent space. CRAFT [29] strengthened the globality and semantic stability of features by leveraging semantic smoothing Transformer layers. GAFlow [22] added Gaussian attention to the existing Transformer block to emphasize local attributes during representation learning, highlight local neighborhoods containing fine-grained structural information, and strengthen motion affinity during matching. In addition, many models took advantage of the Transformer’s global modeling capabilities, adopting a global matching strategy to avoid multiple iterations of refinement, significantly enhancing efficiency. GMFlow [36] reformulated the optical flow problem as a global matching problem and obtained the optical flow using one-time global matching, which was more accurate and faster. Transflow [21] used spatial self-attention and cross-attention mechanisms between adjacent frames to effectively capture global dependencies, providing more accurate correlations and reliable matches in flow estimation. Still, despite these advances in accuracy, the Transformer-based optical flow methods face challenges due to the quadratic complexity of the attention mechanism led to huge computational complexity and memory requirements. This slows inference speed and restricts their use in resource-limited settings, creating practical bottlenecks.

In our proposed MambaFlow architecture, we employ the Mamba module, which contains linear complexity and discriminative feature representation. This approach significantly reduces the overhead of computational resources and memory requirements while maintaining high accuracy comparable to Transformer-based methods, A remarkable breakthrough for the practical application of optical flow models.

2.2. State Space Model in Optical Flow

State space models [7], which originated from control theory, have been effectively integrated with deep learning to capture long-range dependencies. Mamba [5] introduced an input adaptation mechanism to enhance the state space model, providing faster inference speed, higher throughput and overall indicators compared to the Transformers of the same size, especially in natural language. Related work on Mamba [33] has shown that it has comparable performance to the Transformer-based methods while significantly reducing computational complexity. This superiority led to further exploration like Vision Mamba [44] and Vmamba [20], which applied SSMs to visual tasks such as image classification [20, 44], video understanding [17, 32], biomedical image segmentation [23, 35] and others [9, 12, 26, 27, 39]. However, their applicability to optical flow estimation remained unclear until recently. Lin

et al. [18] pioneered Mamba into the scene flow estimation task, proposing an SSM-based iterative update module to replace the GRU module as a decoder. This approach can effectively integrate global motion information in the point cloud and significantly improved inference speed.

Inspired by the Mamba’s linear complexity, we propose a Mamba-centric optical flow estimation architecture, aiming to replace the traditional attention mechanism and thus improve computational efficiency of the model. In this work, we explore the potential of Mamba for modeling sequential interactions in optical flow tasks and propose FEM module and FPM module. The FEM module enhances the features from pairs of images, capturing the dependency between them, while the FPM module refines optical flow predictions for occluded pixels by leveraging both the optical flow field and image structure similarity. By utilizing Mamba’s linear time complexity, our approach overcomes the quadratic complexity limitations of traditional Transformer models when processing long sequences, resulting in significantly improved inference efficiency.

3. Method

3.1. Preliminaries

SSMs are inspired by linear systems, mapping an input sequence $x_t \in \mathbb{R}$ to an output $y_t \in \mathbb{R}$ through a hidden state $h_t \in \mathbb{R}^N$. The model can be formulated as linear ordinary differential equations (ODEs):

$$h_t = \bar{\mathbf{A}}h_{t-1} + \bar{\mathbf{B}}x_t, \quad (1)$$

$$y_t = \mathbf{C}h_t, \quad (2)$$

where $\bar{\mathbf{A}}$ and $\bar{\mathbf{B}}$ represent the discretized parameters derived from the given parameters $\mathbf{A} \in \mathbb{R}^{N \times N}$, $\mathbf{B} \in \mathbb{R}^{N \times 1}$, and the time scale parameter Δ :

$$\bar{\mathbf{A}} = \exp(\Delta \mathbf{A}), \quad (3)$$

$$\bar{\mathbf{B}} = (\Delta \mathbf{A})^{-1}(\exp(\Delta \mathbf{A}) - \mathbf{I}) \cdot \Delta \mathbf{B}. \quad (4)$$

Additionally, $\mathbf{C} \in \mathbb{R}^{1 \times N}$ serves as the projection matrix mapping the hidden state h_t to the output y_t .

Finally, the models generate the output using a global convolution operation, defined as:

$$\bar{\mathbf{K}} = (\mathbf{C}\bar{\mathbf{B}}, \mathbf{C}\bar{\mathbf{A}}\bar{\mathbf{B}}, \dots, \mathbf{C}\bar{\mathbf{A}}^{M-1}\bar{\mathbf{B}}), \quad (5)$$

$$y = x * \bar{\mathbf{K}}, \quad (6)$$

where M represents the length of the input sequence x , and $\bar{\mathbf{K}} \in \mathbb{R}^M$ denotes a structured convolutional kernel.

The recently proposed advanced state-space model, Mamba, enhances \mathbf{B} , \mathbf{C} , and Δ by making them input-dependent, thereby enabling dynamic feature representations. Specifically, these matrices are defined as follows:

$$\mathbf{B}_i = S_B(x_i), \quad (7)$$

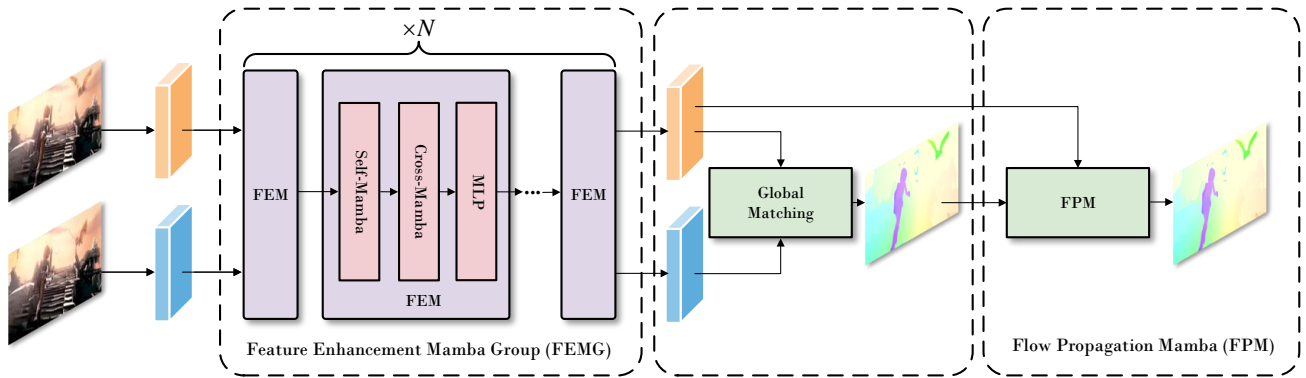


Figure 2. **The overall network architecture of our MambaFlow.** First, we perform downsampling using convolutional layers and input the initially extracted features into the feature enhancement Mamba group (FEMG) module, which is composed of multiple feature enhancement Mamba (FEM) module. Each FEM module consists of Self-Mamba, Cross-Mamba, and MLP for feature enhancement. Next, global matching is applied to the output feature matrix for similarity matching, and the original optical flow is obtained through a softmax layer. Finally, the flow propagation Mamba (FPM) module is used to address inaccuracies in optical flow prediction caused by occlusion.

$$\mathbf{C}_i = S_C(x_i), \quad (8)$$

$$\Delta_i = \text{Softplus}(S_\Delta(x_i)), \quad (9)$$

where S_B , S_C , and S_Δ are linear projection functions, and i denotes the index of the i -th element in the sequence.

Simultaneously, the parallel scan algorithm enables Mamba to leverage the same parallel processing advantages as described in (5), thereby facilitating efficient training.

3.2. Overall Architecture

Optical flow can be intuitively understood as a task aimed at finding pixel-wise correspondences between images. As shown in Fig. 2, our MambaFlow consists of three components: feature enhancement Mamba, global matching and flow propagation Mamba.

Given two consecutive frames \mathbf{I}_1 and \mathbf{I}_2 , we apply a shared-weight convolutional neural network to perform downsampling, obtaining dense feature maps $\mathbf{F}_1, \mathbf{F}_2 \in \mathbb{R}^{H \times W \times D}$. Here, H , W , and D denote the height, width, and feature dimension of the feature maps, respectively. Next, the image features are processed through the feature enhancement stage to obtain the enhanced features of the l -th layer, \mathbf{F}_q and $\mathbf{F}_v \in \mathbb{R}^{H \times W \times D}$. This stage is composed of multiple stacked FEM modules, each consisting of Self-Mamba and Cross-Mamba blocks. Additionally, a Multi-Layer Perceptron (MLP) layer is introduced at the end of each group to further integrate local and global features and enhance feature representation. Finally, we employ the Global Matching method to predict optical flow and use our FPM module to significantly improve performance in occluded regions.

3.3. Self-Mamba

The input features $\mathbf{F}_1, \mathbf{F}_2 \in \mathbb{R}^{H \times W \times D}$ are enriched with learnable positional embeddings to retain spatial posi-

tional information. Subsequently, \mathbf{F}_1 and \mathbf{F}_2 are processed through a weight-sharing Self-Mamba block, generating x_q and x_v , respectively.

As shown in Fig. 3 (a), the processing within each Self-Mamba block can be summarized as a bidirectional operation, where the forward and backward hidden states are computed and combined to enrich the feature representation. The overall process is expressed as:

$$\begin{aligned} y &= \text{Self-Mamba}(x) \\ &= \text{Self-Forward}(x) + \text{Self-Backward}(x). \end{aligned} \quad (10)$$

Here, the Self-Mamba function represents the state space model used to compute the forward and backward hidden states, with the sequence x being reversed to distinguish between the forward and backward directions.

3.4. Cross-Mamba

Mamba is specifically designed to capture long-term dependencies within a single sequence, but it cannot model the interrelations between two sets as effectively as the cross-attention mechanism in the Transformers. To overcome this limitation, we propose Cross-Mamba, an extension of the Mamba framework that adapts the cross-attention mechanism to better capture the interactions between two distinct sets. This idea, which builds upon the work by [33], is further extended in our approach. Since the parameters $\bar{\mathbf{A}}$, $\bar{\mathbf{B}}$, \mathbf{C} , and Δ are associated with the input, $\bar{\mathbf{K}}$ in (5) is extended into an $M \times M$ matrix [1]. The element $\alpha_{i,j}$, located at row i and column j , is determined as follows:

$$\alpha_{i,j} = \mathbf{C}_i \prod_{k=j+1}^i \bar{\mathbf{A}}_k \bar{\mathbf{B}}_j. \quad (11)$$

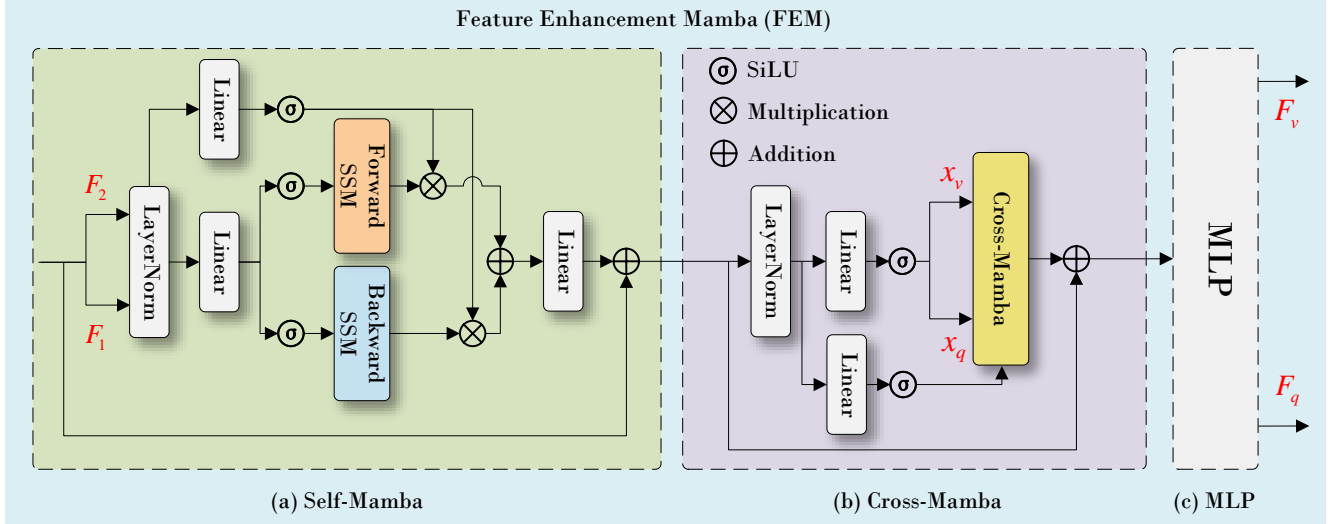


Figure 3. **The architecture of feature enhancement Mamba (FEM) module.** It consists of three core components: Self-Mamba (a), which focuses on a single feature input, Cross-Mamba (b), which handles the interaction between two features, and MLP (c), which performs non-linear feature transformation.

Substituting the equations from (3) to (9), we can ultimately derive the output of Mamba as follows:

$$y_i = \sum_{j=1}^i \alpha_{i,j} x_j = \sum_{j=1}^i Q_i K_j H_{i,j} V_j, \quad (12)$$

where

$$Q_i = S_C(x_i), \quad (13)$$

$$\begin{aligned} K_j &= (\text{Softplus}(S_\Delta(x_j)) \mathbf{A})^{-1} \\ &= (\exp(\text{Softplus}(S_\Delta(x_j)) \mathbf{A}) - \mathbf{I}) \\ &= (\text{Softplus}(S_\Delta(x_j)) S_B(x_j)), \end{aligned} \quad (14)$$

$$H_{i,j} = \prod_{k=j+1}^i \exp(\text{Softplus}(S_\Delta(x_k)) \mathbf{A}), \quad (15)$$

$$V_i = x_i. \quad (16)$$

Cross-attention is a crucial mechanism for modeling the relationships between two sets. It operates by computing interactions between the query (Q) from one set and the keys (K) and values (V) from another set, thereby identifying and focusing on the most relevant elements in the target set. By applying x_q to (13), and x_v to (14), (15) and (16), respectively, Cross-Mamba can be expressed in the following form:

$$y_i = \sum_{j=1}^i f_{m,q}(x_{q,i}) f_{m,k}(x_{v,j}) H_{i,j} x_{v,j}. \quad (17)$$

Cross-Mamba extends the original Mamba by expanding its application from a single input sequence to two input sequences, as shown in Fig. 3 (b). It is formally defined as follows:

$$y = \text{Cross-Mamba}(x_q, x_v). \quad (18)$$

Similarly, we introduce the bidirectional mechanism of Self-Mamba into Cross-Mamba. The formulation is expressed as follows:

$$\begin{aligned} y &= \text{Cross-Mamba}(x_q, x_v) \\ &= \text{Cross-Forward}(x_q, x_v) + \\ &\quad \text{Cross-Backward}(x_q, x_v). \end{aligned} \quad (19)$$

3.5. Global Matching

After extracting the enhanced features \mathbf{F}_q and \mathbf{F}_v from our FEM module, we construct a 4D cost volume of size $H \times W \times H \times W$ by computing the dot-product similarity between all pixel pairs from both features. The construction process is expressed as:

$$\mathbf{C} = \frac{\mathbf{F}_q \mathbf{F}_v^\top}{\sqrt{D}}, \quad (20)$$

where D is the feature dimension. The constructed 4D cost volume can be interpreted as a collection of $H \times W$ 2D cost maps, where each map evaluates the feature similarity between a single pixel in \mathbf{F}_q and all pixels in \mathbf{F}_v . To obtain a matching distribution, a softmax operation is applied across the last two dimensions of the cost volume:

$$\mathbf{M} = \text{softmax}(\mathbf{C}). \quad (21)$$

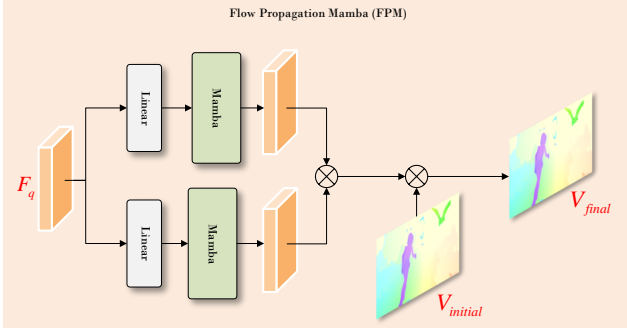


Figure 4. The architecture of flow propagation Mamba (FPM) module.

To estimate the optical flow, the correspondence $\hat{\mathbf{G}}$ is obtained by taking a weighted average of the 2D pixel grid coordinates $\mathbf{G} \in \mathbb{R}^{H \times W \times 2}$ in the target image with the matching distribution M :

$$\hat{\mathbf{G}} = \mathbf{M}\mathbf{G}. \quad (22)$$

Finally, the optical flow $\mathbf{V}_{\text{original}}$ is calculated as the difference between the corresponding pixel coordinates:

$$\mathbf{V}_{\text{original}} = \hat{\mathbf{G}} - \mathbf{G}. \quad (23)$$

The global matching method effectively improves the accuracy and stability of optical flow estimation by capturing global contextual information.

3.6. Flow Propagation Mamba

To address the issue of occluded regions or pixels outside the image boundaries, we introduced a self-similarity-based module called the flow propagation Mamba (FPM) module (as illustrated in Fig. 4), which leverages feature information from the source image to capture pixel-level similarity relationships. Since adjacent pixels typically exhibit similar features, they demonstrate higher similarity, thus providing a more robust solution for optical flow estimation. Specifically, by inputting \mathbf{F}_q into the Mamba block, we enhance the features in occluded regions and further extract the weights of these occluded areas. This helps optimize the final optical flow estimation, thereby improving accuracy and robustness in complex scenarios. The formula is as follows:

$$\mathbf{V}_{\text{final}} = \text{softmax}(\text{Mamba}(\mathbf{F}_q)) \mathbf{V}_{\text{initial}}, \quad (24)$$

where $\mathbf{V}_{\text{initial}} \in \mathbb{R}^{H \times W \times 2}$ represents the optical flow predicted by the global matching.

4. Experiments

Datasets. Following the previous methodology, we first pre-train on the FlyingChairs (Chairs)[4] and FlyingThings3D (Things)[24] datasets. For fine-tuning, we adopt a

mixed training set consisting of KITTI [25], HD1K [16], FlyingThings3D, and Sintel [2] training sets. Finally, we further fine-tune the model on the KITTI training set and report the performance on the respective online benchmarks.

Metrics. In our experiments, we employed evaluation metrics commonly used in optical flow estimation. Firstly, we utilized the end-point-error (EPE) to measure the average Euclidean distance between the predicted and ground truth optical flow vectors. For the KITTI dataset, we adopted the F1-all metric, which represents the percentage of pixels with an error exceeding 3 pixels or a relative error greater than 5%. To gain deeper insights into the model’s performance under large motion magnitudes, we defined s_{40+} as the EPE for pixels where the ground truth flow magnitude exceeds 40 pixels.

Implementation Details. Our model is constructed using the PyTorch library and trained on 4 NVIDIA GeForce RTX 3090 GPUs. Following the training strategy from previous works [31, 36], we use the AdamW optimizer. The model is first pre-trained on the Chairs dataset for 100k iterations with a batch size of 16 and a learning rate of 4×10^{-4} . Then, it is fine-tuned on the Things dataset for 200k iterations with a batch size of 8 and a learning rate of 2×10^{-4} . During this process, we select the best-performing model on the Things dataset and fine-tune it for an additional 800k iterations to validate the ablation study. Subsequently, the model fine-tuned for 200k iterations on the Things dataset is used as the initial model and further trained on the Sintel dataset, keeping the same hyperparameters as those used for the Things dataset, including a batch size of 8 and a learning rate of 2×10^{-4} . Finally, we continue training on the KITTI-2015 training set for 200k iterations with the batch size and learning rate unchanged.

4.1. Comparison with State-of-the-Arts

We compared the performance of different optical flow algorithms on the Sintel and KITTI datasets, and the experimental results are shown in Table 1.

Results on Sintel. MambaFlow achieved an EPE of 1.60 on the Sintel Clean dataset and an EPE of 2.78 on the Final dataset. Fig. 5 presents a qualitative analysis of optical flow estimation, comparing MambaFlow with other state-of-the-art approaches on the Sintel test set. The results show that MambaFlow’s performance on Clean and Final is at the same level as current mainstream methods such as RAFT and GMA, demonstrating its strong adaptability in both simple and complex scenarios.

Results on KITTI. MambaFlow achieves an F1-all score of 8.53% on the KITTI dataset while demonstrating a sig-

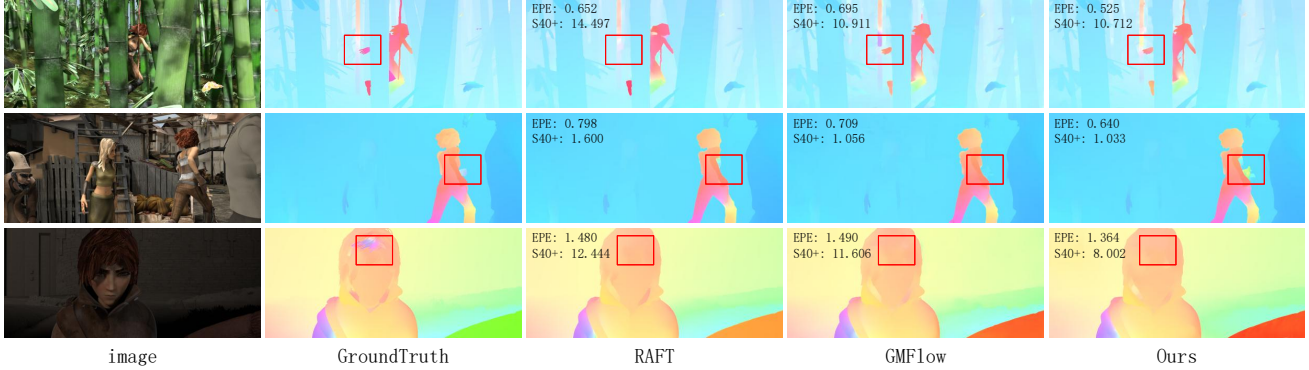


Figure 5. Visual results on Sintel test set.

Training Data	Method	Sintel		KITTI		Inference Cost	
		Clean↓	Final↓	Fl-all↓	Param	Time	
C+T+S+K+H	RAFT [31]	1.61	2.86	5.10	5.3M	140.7ms	
	SeparableFlow [40]	1.50	2.67	4.64	6.0M	229.1ms	
	GMA [15]	1.39	2.47	5.15	5.9M	183.3ms	
	DIP [43]	1.44	2.83	4.21	5.4M	498.9ms	
	GMFlowNet [41]	1.39	2.65	4.79	9.3M	244.3ms	
	CRAFT [29]	1.45	2.42	7.79	6.3M	483.4ms	
	MS-RAFT [13]	1.37	2.67	4.88	13.5M	627.3ms	
	MatchFlow [3]	1.33	2.64	4.72	14.8M	283.8ms	
	MS-RAFT+ [14]	1.23	2.68	4.15	16.0M	1108.2ms	
	GMFlow [36]	1.74	2.90	9.32	4.7M	138.5ms	
	MambaFlow (ours)	1.60	2.78	8.53	8.9M	113.5ms	

Table 1. MambaFlow achieves at least 18% faster inference on the KITTI (test) dataset compared to other state-of-the-art methods with competitive performance. All compared methods were evaluated under the same training configuration, and a unified "C+T+S+K+H" training strategy was adopted to ensure the fairness of the results. For performance measurements, we used the normalized setting of batch size 1 and input resolution 540×960 . In addition, all inference times are measured on the RTX 3090 graphics card. The significant performance improvement highlights MambaFlow's advantages in speed and efficiency. It is worth noting that while maintaining competitive accuracy on the Sintel and KITTI datasets, we have successfully achieved a significant improvement in speed, further verifying the superiority of MambaFlow in the speed-accuracy balance.

nificant advantage in inference speed. Specifically, MambaFlow requires only 113.5ms for inference on an RTX 3090, making it 18.1% faster than GMFlow (138.5ms), which is the fastest among the compared methods. Furthermore, MambaFlow runs 2.5 times faster than MatchFlow (283.8ms) and nearly 10 times faster than MS-RAFT+ (1108.2ms), while maintaining competitive accuracy. This demonstrates that MambaFlow is able to maintain comparable accuracy to mainstream methods while significantly reducing inference time when handling larger and more challenging scenarios.

4.2. Ablation Analysis

Components of FEM. We ablate different Feature Enhancement Mamba components in Table 2. Among them,

Cross-Mamba contributes the most as it models the mutual relationship between two features, a relationship that is otherwise missing in the features extracted from the convolutional backbone. Self-Mamba aggregates contextual cues within the same feature, resulting in an additional performance improvement, and positional information introduces location dependence into the matching process, helping to mitigate ambiguities present in feature-similarity-based matching alone. Removing the Multi-Layer Perceptron (MLP) reduces the number of parameters, but also results in a slight decrease in performance.

Number of FEM layers. We conduct an ablation study on the number of FEM layers, as shown in Table 3. The experiment compares the impact of varying the number of

setup	Things (val)			Sintel (train)			Param (M)	
	Clean↓	EPE	Clean↓	EPE	Final↓	EPE		
full	6.45	-	2.23	-	3.41	-	8.1	-
w/o self	6.89	↑6.8%	2.30	↑3.1%	3.49	↑2.3%	6.9	↓14.8%
w/o cross	11.10	↑72.1%	3.78	↑69.5%	5.16	↑51.3%	4.4	↓45.7%
w/o MLP	7.13	↑10.5%	2.41	↑8.1%	3.66	↑7.3%	5.2	↓35.8%
w/o pos	6.65	↑3.1%	2.29	↑2.7%	3.48	↑2.1%	8.1	-

Table 2. **FEM components.** Ablation study on individual components, revealing that Cross-Mamba contributes the most.

layers	Sintel (train)		KITTI (train)		Param (M)
	Clean↓	Final↓	EPE↓	F1-all↓	
4	1.41	2.79	9.53	27.15	5.1
6	1.37	2.72	9.16	25.38	6.9
8	1.36	2.63	8.54	24.97	8.9
10	1.35	2.68	8.51	24.67	10.8
12	1.36	2.55	8.10	23.91	12.7
24	1.34	2.50	7.96	22.97	23.4

Table 3. **Number of Mamba layers.** Using 8 layers of Mamba strikes an optimal balance between accuracy and parameter efficiency.

training iterations	Things (val)		Sintel (train)		KITTI (train)	
	Clean↓	Final↓	Clean↓	Final↓	EPE↓	F1-all↓
200K	3.04	1.19	2.60	9.02	25.92	
400K	2.81	1.14	2.57	8.76	25.18	
600K	2.73	1.10	2.52	8.14	24.18	
800K	2.61	1.09	2.56	7.57	23.51	

Table 4. **Training iterations.** MambaFlow benefits from more training iterations.

FEM layers on overall performance. Among all the tested configurations, the FEMG module with 8 Mamba layers exhibits the best performance.

Training iterations. The experimental results in Table 4 show that with the increase in the number of training iterations, our framework has achieved certain improvements in performance. This shows that more training iterations can effectively improve the performance of the model, making it more stable and accurate in subsequent tasks.

5. Conclusion

In this paper, we explore for the first time the application of the advanced Mamba in optical flow estimation, and then propose a simple, accurate and efficient Mamba-centric optical flow method, MambaFlow, for end-to-end flow predic-

tion. It consists of two components built on Mamba architecture: the FEM module and FPM module. The FEM is proposed for accurate and efficient feature enhancement, incorporating the Self-Mamba, Cross-Mamba mechanisms to tackle the issue of inadequate feature representation. Furthermore, the FPM that employs feature self-similarity to direct the ultimate flow is crafted for the flow propagation, addressing the challenge of traditional recurrent refined methods. Our method achieves comparable accuracy to state-of-the-art algorithms while significantly reducing inference time, with a runtime of 0.113 seconds—18% faster than GMFlow and 10 times faster than MS-RAFT+. We attribute this to the high accuracy and efficiency of Mamba in capturing features with local correlation while maintaining its global information. As far as we know, this is the first Mamba-centric architecture designed for end-to-end optical flow estimation. We are assured that additional variants of the Mamba-centric methods may emerge, possessing significant potential to boost both precision and velocity in the future.

References

- [1] Ameen Ali, Itamar Zimerman, and Lior Wolf. The hidden attention of mamba models. *arXiv preprint arXiv:2403.01590*, 2024. 4
- [2] Daniel J Butler, Jonas Wulff, Garrett B Stanley, and Michael J Black. A naturalistic open source movie for optical flow evaluation. In *Computer Vision–ECCV 2012: 12th European Conference on Computer Vision, Florence, Italy, October 7–13, 2012, Proceedings, Part VI 12*, pages 611–625. Springer, 2012. 6
- [3] Qiaole Dong, Chenjie Cao, and Yanwei Fu. Rethinking optical flow from geometric matching consistent perspective, 2023. 7
- [4] Alexey Dosovitskiy, Philipp Fischer, Eddy Ilg, Philip Hausser, Caner Hazirbas, Vladimir Golkov, Patrick Van Der Smagt, Daniel Cremers, and Thomas Brox. Flownet: Learning optical flow with convolutional networks. In *Proceedings of the IEEE international conference on computer vision*, pages 2758–2766, 2015. 1, 2, 6
- [5] Albert Gu and Tri Dao. Mamba: Linear-time sequence modeling with selective state spaces. *arXiv preprint arXiv:2312.00752*, 2023. 2, 3

[6] Albert Gu, Isys Johnson, Karan Goel, Khaled Saab, Tri Dao, Atri Rudra, and Christopher Ré. Combining recurrent, convolutional, and continuous-time models with linear state space layers. *Advances in neural information processing systems*, 34:572–585, 2021. 2

[7] Albert Gu, Karan Goel, and Christopher Ré. Efficiently modeling long sequences with structured state spaces, 2022. 3

[8] Berthold KP Horn and Brian G Schunck. Determining optical flow. *Artificial intelligence*, 17(1-3):185–203, 1981. 2

[9] Vincent Tao Hu, Stefan Andreas Baumann, Ming Gui, Olga Grebenkova, Pingchuan Ma, Johannes Fischer, and Björn Ommer. Zigma: A dit-style zigzag mamba diffusion model. In *European Conference on Computer Vision*, pages 148–166. Springer, 2025. 3

[10] Zhaoyang Huang, Xiaoyu Shi, Chao Zhang, Qiang Wang, Ka Chun Cheung, Hongwei Qin, Jifeng Dai, and Hongsheng Li. Flowformer: A transformer architecture for optical flow. In *European conference on computer vision*, pages 668–685. Springer, 2022. 2, 3

[11] Zhewei Huang, Tianyuan Zhang, Wen Heng, Boxin Shi, and Shuchang Zhou. Real-time intermediate flow estimation for video frame interpolation. In *European Conference on Computer Vision*, pages 624–642. Springer, 2022. 1

[12] Md Mohaiminul Islam, Mahmudul Hasan, Kishan Shamsundar Athrey, Tony Braskich, and Gedas Bertasius. Efficient movie scene detection using state-space transformers. In *Proceedings of the IEEE/CVF Conference on Computer Vision and Pattern Recognition*, pages 18749–18758, 2023. 3

[13] Azin Jahedi, Lukas Mehl, Marc Rivinius, and Andrés Bruhn. Multi-scale raft: Combining hierarchical concepts for learning-based optical flow estimation. In *2022 IEEE International Conference on Image Processing (ICIP)*, pages 1236–1240. IEEE, 2022. 7

[14] Azin Jahedi, Maximilian Luz, Marc Rivinius, Lukas Mehl, and Andrés Bruhn. Ms-raft+: High resolution multi-scale raft. *International Journal of Computer Vision*, 132(5):1835–1856, 2024. 7

[15] Shihao Jiang, Dylan Campbell, Yao Lu, Hongdong Li, and Richard Hartley. Learning to estimate hidden motions with global motion aggregation. In *Proceedings of the IEEE/CVF international conference on computer vision*, pages 9772–9781, 2021. 2, 7

[16] Daniel Kondermann, Rahul Nair, Katrin Honauer, Karsten Krispin, Jonas Andrusis, Alexander Brock, Burkhard Gussfeld, Mohsen Rahimimoghadam, Sabine Hofmann, Claus Brenner, et al. The hci benchmark suite: Stereo and flow ground truth with uncertainties for urban autonomous driving. In *Proceedings of the IEEE Conference on Computer Vision and Pattern Recognition Workshops*, pages 19–28, 2016. 6

[17] Kunchang Li, Xinhao Li, Yi Wang, Yinan He, Yali Wang, Limin Wang, and Yu Qiao. Videomamba: State space model for efficient video understanding. In *European Conference on Computer Vision*, pages 237–255. Springer, 2025. 3

[18] Min Lin, Gangwei Xu, Yun Wang, Xianqi Wang, and Xin Yang. Flowmamba: Learning point cloud scene flow with global motion propagation. *arXiv preprint arXiv:2412.17366*, 2024. 3

[19] Xiaozhang Liu, Hui Liu, and Yuxiu Lin. Video frame interpolation via optical flow estimation with image inpainting. *International Journal of Intelligent Systems*, 35(12):2087–2102, 2020. 1

[20] Yue Liu, Yunjie Tian, Yuzhong Zhao, Hongtian Yu, Lingxi Xie, Yaowei Wang, Qixiang Ye, Jianbin Jiao, and Yunfan Liu. Vmamba: Visual state space model, 2024. 3

[21] Yawen Lu, Qifan Wang, Siqi Ma, Tong Geng, Yingjie Victor Chen, Huajin Chen, and Dongfang Liu. Transflow: Transformer as flow learner. In *Proceedings of the IEEE/CVF conference on computer vision and pattern recognition*, pages 18063–18073, 2023. 3

[22] Ao Luo, Fan Yang, Xin Li, Lang Nie, Chunyu Lin, Haoqiang Fan, and Shuaicheng Liu. Gaflow: Incorporating gaussian attention into optical flow. In *Proceedings of the IEEE/CVF International Conference on Computer Vision*, pages 9642–9651, 2023. 3

[23] Jun Ma, Feifei Li, and Bo Wang. U-mamba: Enhancing long-range dependency for biomedical image segmentation. *arXiv preprint arXiv:2401.04722*, 2024. 3

[24] Nikolaus Mayer, Eddy Ilg, Philip Hausser, Philipp Fischer, Daniel Cremers, Alexey Dosovitskiy, and Thomas Brox. A large dataset to train convolutional networks for disparity, optical flow, and scene flow estimation. In *Proceedings of the IEEE conference on computer vision and pattern recognition*, pages 4040–4048, 2016. 6

[25] Moritz Menze and Andreas Geiger. Object scene flow for autonomous vehicles. In *Proceedings of the IEEE conference on computer vision and pattern recognition*, pages 3061–3070, 2015. 6

[26] Eric Nguyen, Karan Goel, Albert Gu, Gordon Downs, Preey Shah, Tri Dao, Stephen Baccus, and Christopher Ré. S4nd: Modeling images and videos as multidimensional signals with state spaces. *Advances in neural information processing systems*, 35:2846–2861, 2022. 3

[27] Shiyu Qin, Jinpeng Wang, Yimin Zhou, Bin Chen, Tianci Luo, Baoyi An, Tao Dai, Shutao Xia, and Yaowei Wang. Mambavc: Learned visual compression with selective state spaces. *arXiv preprint arXiv:2405.15413*, 2024. 3

[28] Anurag Ranjan and Michael J Black. Optical flow estimation using a spatial pyramid network. In *Proceedings of the IEEE conference on computer vision and pattern recognition*, pages 4161–4170, 2017. 2

[29] Xiuchao Sui, Shaohua Li, Xue Geng, Yan Wu, Xinxing Xu, Yong Liu, Rick Goh, and Hongyuan Zhu. Craft: Cross-attentional flow transformer for robust optical flow. In *Proceedings of the IEEE/CVF conference on Computer Vision and Pattern Recognition*, pages 17602–17611, 2022. 3, 7

[30] Deqing Sun, Xiaodong Yang, Ming-Yu Liu, and Jan Kautz. Pwc-net: Cnns for optical flow using pyramid, warping, and cost volume. In *Proceedings of the IEEE conference on computer vision and pattern recognition*, pages 8934–8943, 2018. 1, 2

[31] Zachary Teed and Jia Deng. Raft: Recurrent all-pairs field transforms for optical flow. In *Computer Vision–ECCV 2020: 16th European Conference, Glasgow, UK, August 23–28, 2020, Proceedings, Part II 16*, pages 402–419. Springer, 2020. 1, 2, 6, 7

- [32] Jue Wang, Wentao Zhu, Pichao Wang, Xiang Yu, Linda Liu, Mohamed Omar, and Raffay Hamid. Selective structured state-spaces for long-form video understanding. In *Proceedings of the IEEE/CVF Conference on Computer Vision and Pattern Recognition*, pages 6387–6397, 2023. [3](#)
- [33] Donghang Wu, Yiwen Wang, Xihong Wu, and Tianshu Qu. Cross-attention inspired selective state space models for target sound extraction, 2024. [3](#), [4](#)
- [34] Song Wu, Kaichao You, Weihua He, Chen Yang, Yang Tian, Yaoyuan Wang, Ziyang Zhang, and Jianxing Liao. Video interpolation by event-driven anisotropic adjustment of optical flow. In *European Conference on Computer Vision*, pages 267–283. Springer, 2022. [1](#)
- [35] Zhaohu Xing, Tian Ye, Yijun Yang, Guang Liu, and Lei Zhu. Segmamba: Long-range sequential modeling mamba for 3d medical image segmentation. In *International Conference on Medical Image Computing and Computer-Assisted Intervention*, pages 578–588. Springer, 2024. [3](#)
- [36] Haofei Xu, Jing Zhang, Jianfei Cai, Hamid Rezatofighi, and Dacheng Tao. Gmflow: Learning optical flow via global matching. In *Proceedings of the IEEE/CVF conference on computer vision and pattern recognition*, pages 8121–8130, 2022. [2](#), [3](#), [6](#), [7](#)
- [37] Xiangyu Xu, Li Siyao, Wenxiu Sun, Qian Yin, and Ming-Hsuan Yang. Quadratic video interpolation. *Advances in Neural Information Processing Systems*, 32, 2019. [1](#)
- [38] Zhonghua Yi, Hao Shi, Kailun Yang, Qi Jiang, Yaozu Ye, Ze Wang, Huajian Ni, and Kaiwei Wang. Focusflow: Boosting key-points optical flow estimation for autonomous driving. *IEEE Transactions on Intelligent Vehicles*, 2023. [1](#)
- [39] Yaohua Zha, Naiqi Li, Yanzi Wang, Tao Dai, Hang Guo, Bin Chen, Zhi Wang, Zhihao Ouyang, and Shu-Tao Xia. Lcm: Locally constrained compact point cloud model for masked point modeling. *arXiv preprint arXiv:2405.17149*, 2024. [3](#)
- [40] Feihu Zhang, Oliver J Woodford, Victor Adrian Prisacariu, and Philip HS Torr. Separable flow: Learning motion cost volumes for optical flow estimation. In *Proceedings of the IEEE/CVF international conference on computer vision*, pages 10807–10817, 2021. [2](#), [7](#)
- [41] Shiyu Zhao, Long Zhao, Zhixing Zhang, Enyu Zhou, and Dimitris Metaxas. Global matching with overlapping attention for optical flow estimation, 2022. [7](#)
- [42] Yuxuan Zhao, Ka Lok Man, Jeremy Smith, Kamran Siddiqie, and Sheng-Uei Guan. Improved two-stream model for human action recognition. *EURASIP Journal on Image and Video Processing*, 2020:1–9, 2020. [1](#)
- [43] Zihua Zheng, Ni Nie, Zhi Ling, Pengfei Xiong, Jiangyu Liu, Hao Wang, and Jiankun Li. Dip: Deep inverse patchmatch for high-resolution optical flow, 2022. [7](#)
- [44] Lianghui Zhu, Bencheng Liao, Qian Zhang, Xinlong Wang, Wenyu Liu, and Xinggang Wang. Vision mamba: Efficient visual representation learning with bidirectional state space model. *arXiv preprint arXiv:2401.09417*, 2024. [3](#)